Hindawi
Mathematical Problems in Engineering
Volume 2017, Article ID 7421842, 10 pages
https://doi.org/10.1155/2017/7421842

Research Article

A Hot Spots Ignition Probability Model for Low-Velocity Impacted Explosive Particles Based on the Particle Size and Distribution

Hong-fu Guo, Yan-qing Wu, and Feng-lei Huang

State Key Laboratory of Explosion Science and Technology, Beijing Institute of Technology, Beijing 100081, China

Correspondence should be addressed to Yan-qing Wu; 3120140066@bit.edu.cn and Feng-lei Huang; huangfl@bit.edu.cn

Received 15 July 2016; Revised 7 November 2016; Accepted 28 November 2016; Published 8 February 2017

Academic Editor: Michael Vynnycky

Particle size and distribution play an important role in ignition. The size and distribution of the cyclotetramethylene tetranitramine (HMX) particles were investigated by Laser Particle Size Analyzer Malvern MS2000 before experiment and calculation. The mean size of particles is 161 μm. Minimum and maximum sizes are 80 μm and 263 μm, respectively. The distribution function is like a quadratic function. Based on the distribution of micron scale explosive particles, a microscopic model is established to describe the process of ignition of HMX particles under drop weight. Both temperature of contact zones and ignition probability of powder explosive can be predicted. The calculated results show that the temperature of the contact zones between the particles and the drop weight surface increases faster and higher than that of the contact zones between two neighboring particles. For HMX particles, with all other conditions being kept constant, if the drop height is less than 0.1 m, ignition probability will be close to 0. When the drop heights are 0.2 m and 0.3 m, the ignition probability is 0.27 and 0.64, respectively, whereas when the drop height is more than 0.4 m, ignition probability will be close to 0.82. In comparison with experimental results, the two curves are reasonably close to each other, which indicates our model has a certain degree of rationality.

1. Introduction

Impact sensitivity of energetic materials is one of the most important safety concerns in engineering applications. The drop weight test is the simplest and most commonly used method to assess the sensitivity of explosives [1, 2]. It is generally believed that hot spot formation plays an important role in determining impact sensitivity of energetic materials. However, the physical mechanisms responsible for hot spot formation under drop weight impact remain unresolved.

In Cavendish laboratory, Heavens and Field [3] modified the drop weight machine to allow high-speed photography to observe the dynamic compression events of granular explosives. Czerski et al. [4] designed a set of test devices, using high-speed photography and second harmonic detection technology (SHG) to study the ignition behavior of HMX under the impact; they found a little of delta-phase HMX before the ignition, which proved the drop weight impact on HMX sample can cause HMX phase to change. Drop weight impact testing shows that HMX microcrystals of nanoscale size are much less sensitive than HMX bulk crystals [5]. Wu and Huang [6] have used high-speed photography to record the impact response behavior of the monolayer HMX particles under drop weight and analyzed its ignition mechanism. An et al. [7] found that the mechanical sensitivity of HMX reduces obviously if it covered with HTPB. The thermal impact sensitivities of PETN, TATP, HMX, and silver azide (AgN_3) as a function of temperature are obtained [8]. In theoretical investigations, many computational models are established. Namkung and Coffey [9] found plastic energy deposition rate of solid is related to the deformation rate; plastic deformation caused local deposition of energy in explosive crystals due to mild shock or impact and then triggered a chemical reaction. Keshavarz and Jaafari [10] introduced a generalized scheme for predicting impact sensitivity of any explosives by using artificial neural networks in 2006.

A micromechanics approach based on heating equations and the kinematic and deformation description for a thin layer of HMX energetic powders under drop weight impact is established; the work focuses on the thermal and mechanical processes that act to transfer the input kinetic energy into the localized high-temperature ignition sites [11]. Wu et al. [12–14] established some microscopic hot spot model, and they used those model to explain explosives thermodynamic performance under low-velocity impact. In multiple phase processes, interphase heat exchange plays the role of heat losses in homogeneous combustible gas mixtures. Adegbie and Alao [15] established a mathematical model to examine the effects of interphase heat exchange between the gas and solid particles. The model with heat losses provides more detailed information about the effects of interphase heat exchange and numeric exponent characterizing sensitized, Arrhenius, and bimolecular rate of reactions. Jankowski's model investigated the heterogeneous mixture combustion of liquid fuels and researched processes of spraying and combustion [16]. Numerical and experimental investigations were executed for determination of macroscopic regularities of heat and mass transfer processes under the conditions of the phase transformations and chemical reactions [17]. The physical and forecasting mathematical models about heat and mass transfer with phase transformations and chemical reactions under heating and following ignition of typical liquid fuel were developed [18]. Nemoda et al. [19] established a two-dimensional CFD model of liquid fuel combustion taking into account the third liquid phase, as well as its interaction with the solid and gas phase.

The above researches about ignition of explosive particles did not consider the size and distribution of the particles in the process of the hot spot formation under drop weight. This paper develops a mesoscopic dynamic theory model on the basis of Wu and Huang's model [13] by analyzing the size and distribution of the particles to illustrate the hot spots formation and ignition probability. We first of all investigated the size and distribution of the particles by Laser Particle Size Analyzer Malvern MS2000 before the experiment and calculation. Secondly, we calculated the plastic work and frictional heat of the contact points between particles and between the particles and the drop weight surface and obtained the temperature of the contact points. Finally, we got the ignition probability of explosive particles. The model may provide useful information about safety and sensitivity prediction of energetic materials.

2. Model Description

2.1. Particle Size and Distribution. For HMX particles, particle size is different under the same production method. In this paper, HMX samples were prepared by ball milling methods provided by the China Academy of Engineering Physics and characterized by Laser Particle Size Analyzer Malvern MS2000. The investigation results are shown in Figure 1. The mean size of particles is 161 μm. Minimum and maximum sizes are 80 μm and 263 μm, respectively. In this paper, the weight of the powder explosive is 6.0 mg in experiment and calculation.

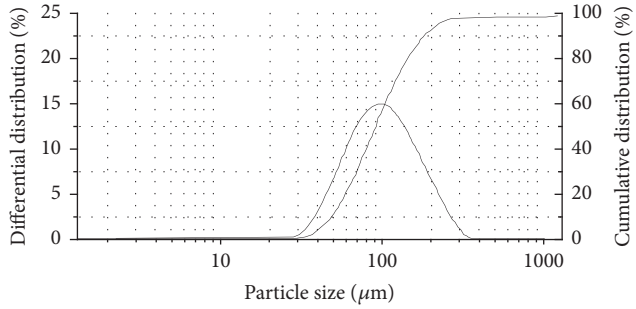

Figure 1: The particle size distribution of HMX.

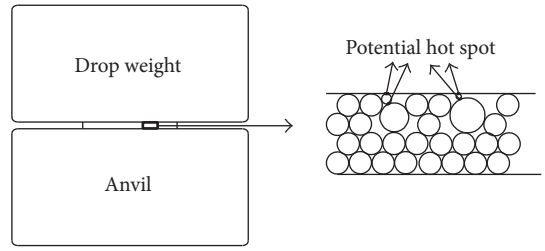

Figure 2: The left represented the drop weight impact at the macroscopic scale; the right represented the potential hot spot sources at the microscopic scale.

2.2. The Kinematics and Dynamic Model. During the process of impact, the contact areas between particles and between the particles and the drop weight surface become potential "hot spots" due to plastic work and frictional heat. The sample is assumed to be spherical particle in the model. Figure 2 represents the macroscopic and microscopic scale kinematics and dynamic model and the potential hot spot sources.

To simplify the calculations, the sample is assumed to consist of two layers. The average size of the particles is $\overline{d}_0 = 161\,\mu$m. Centered on the average size, the particles are divided into eight ranges. The number of particles in each range is N_i $(i = 1, 2, \ldots, 8)$, respectively. The total number of particles is N. The size and number of the particle are shown in Table 1.

For the calculation convenience, we assume the particles are vertical contact firstly. Then we obtained the relationship between force and displacement in nonvertical contact. Figures 3(a) and 3(b) represent the contact model.

As shown in Figure 3(a) the change of the sample thickness arises from the difference between the falling distance of the drop weight x_u and the falling distance of the anvil base. The anvil base can be regarded as rigid and infinite. Thus, $h(t)$ can be given by

$$h(t) = h_0 - x_u, \tag{1}$$

where t is the time. Based on Figure 3(a), the falling distance of the upper drop weight is caused by one factor, namely, the impression depth of particles. Thus, the falling distance can be calculated as

$$x_u = \delta_{1is} + \delta_{2is} + \delta_{3ib} + \delta_{4ib}, \tag{2}$$

where δ_{1is}, δ_{2is}, δ_{3ib}, and δ_{4ib} are the impression depth and i represents the range number $(i = 1, 2, \ldots, 8)$. During impact,

Table 1: The size (μm) and number of the particles.

Size range of particles	161~141	141~121	121~101	101~81
Number of small particles	$N_1 = 213$	$N_2 = 314$	$N_3 = 418$	$N_4 = 545$
Average size	171	191	211	231
Mean radius	75.5	65.5	55.5	45.5
Size range of particles	161~181	181~201	201~221	221~241
Number of big particles	$N_5 = 139$	$N_6 = 88$	$N_7 = 52$	$N_8 = 17$
Average size	171	191	211	231
Mean radius	85.5	95.5	105.5	115.5

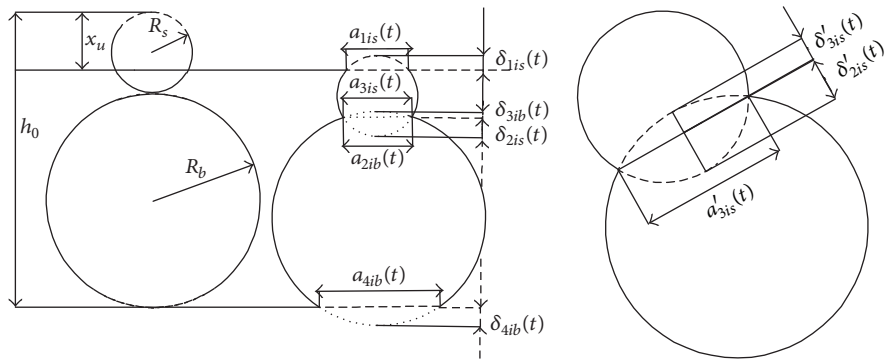

Figure 3: (a) represents the contact model in the vertical contact; (b) represents the contact model in the nonvertical contact.

the motion of the drop weight can be determined from its momentum balance:

$$\ddot{x}_u = g - \frac{F_c(t)}{M_w},$$
$$F_c(t) = \sum_{i=1}^{i=8} \frac{C_{N_i}^1}{C_N^1} F_i(t), \tag{3}$$

where g is the acceleration of gravity, $F_i(t)$ is the force exerted on the drop weight by different range particles, and $F_c(t)$ is the force exerted on the drop weight by all the particles of upper layer. In the early stage, the contact deformation of the particles is elastic which can be described using the Hertz contact theory [20]:

$$F_{i\text{-els}}(t) = \frac{4}{3} E_{\text{eq}} R_{\text{eq}}^{1/2} {\delta_{1is}}^{3/2}, \quad \left(\delta_{1is} < \delta_y,\ \dot{\delta}_{1is} > 0\right), \tag{4}$$

where $F_{i\text{-els}}(t)$ is the elastic force, $R_{\text{eq}} = (1/R_s + 1/R_b)^{-1}$, $E_{\text{eq}} = ((1-v_s^2)/E_s + (1-v_b^2)/E_b)^{-1}$, E is the elastic modulus, v is the Poisson ratio, and R is the radius of the particle.

After the initial yield, the plastic force has a linear relationship with displacement, which is given by Thornton and Ning [21]:

$$F_{i\text{-pla}}(t) = F_y + \pi R_{\text{eq}} \sigma_y \left(\delta_{1is}(t) - \delta_y\right), \quad \left(\delta_y < \delta_{1is},\ \dot{\delta}_{1is} > 0\right), \tag{5}$$

where $F_{i\text{-pla}}(t)$ is the plastic force, F_y is initial yield force, $F_y = (4/3)E_{\text{eq}}R_{\text{eq}}^{1/2}{\delta_y}^{3/2}$, δ_y is the yield impression depth of particle, $\delta_y = (\pi^2 R_{\text{eq}}/4E_{\text{eq}}^2)A_y^2\sigma_y^2$, and σ_y is yield strength of particles.

The average pressure on the particles is given by

$$p_{ci}(t) = \frac{4F_{i\text{-els}}(t)}{\pi a_{1is}^2(t)}, \quad \left(\delta_i < \delta_y\right),$$
$$p_{ci}(t) = \frac{4F_{i\text{-pla}}(t)}{\pi a_{1is}^2(t)}, \quad \left(\delta_y < \delta_i\right). \tag{6}$$

We assume that the volume of the sample is constant in loading process. The sample diameter $d_s(t)$ is related to the sample thickness $h(t)$, and it is given by

$$d_s(t) = \sqrt{\frac{h_0}{h(t)}} d_{s0}. \tag{7}$$

The mean radial velocity is given by Wu and Huang [13]:

$$\overline{v}_p(t) = -\frac{1}{6}\frac{\dot{h}(t)}{h(t)} \cdot d_s(t). \tag{8}$$

The contact radii of particles are $a_{1is}(t)$, $a_{2ib}(t)$, $a_{3is}(t)$, and $a_{4ib}(t)$; they are given by

$$a_{1is}(t) = \frac{R_{is}^{3/2}}{\sqrt{6\left[R_{is} - 2\delta_{1is}(t)\right]}}, \tag{9}$$

$$a_{2is}(t) = \frac{R_{is}^{3/2}}{\sqrt{6\left[R_{is} - 2\delta_{2is}(t)\right]}}, \tag{10}$$

$$a_{3ib}(t) = \frac{R_{ib}^{3/2}}{\sqrt{6\left[R_{ib} - 2\delta_{3ib}(t)\right]}}, \tag{11}$$

$$a_{2is}(t) = a_{3ib}(t), \tag{12}$$

$$a_{4ib}(t) = R_{ib}^{3/2}\sqrt{6\left(R_{ib} - 2\delta_{4ib}\right)}. \tag{13}$$

Assuming that a one-dimensional wave propagates along the loading direction in the particles of the second layer and there is no reflected wave [13, 22], the acceleration of the net depth of the impression on one spherical particle at the first layer is given by Wu and Huang [13]:

$$\ddot{\delta}_{2is}(t) + \ddot{\delta}_{3ib}(t) = -\frac{F(t)}{M_W} - \frac{F_i(t)}{m_p} + \frac{\dot{F}_i(t)}{\rho_s A_s c_s} - \ddot{\delta}_{1is}(t). \tag{14}$$

In the above calculation, we assumed that particles contact is vertical, but the contact between particles is mainly nonvertical contact as shown in Figure 3(b). In this case, the particle can be regarded as a circular disc when the materials are subjected to impact [23, 24]. The impression depths $\dot{\delta}'_{2is}$ and $\dot{\delta}'_{3ib}$, contact forces $F'_{i\text{-els}}$ and $F'_{i\text{-pla}}$, contact radii $a'_{2is}(t)$ and $a'_{3ib}(t)$, and the relative sliding velocity $\overline{v}'_i$ in nonvertical contact are given by Wu and Huang [13]:

$$\begin{aligned}
\dot{\delta}'_{2is}(t) &= \frac{\partial v_p(r,t)}{\partial r}\cdot 2R_{ib}\cdot\cos\theta \\
&= -\frac{\dot{h}(t)}{2h(t)}\cdot 2R_{ib}\cdot\cos\theta, \\
\dot{\delta}'_{3ib}(t) &= \frac{\partial v_p(r,t)}{\partial r}\cdot 2R_{is}\cdot\cos\theta \\
&= -\frac{\dot{h}(t)}{2h(t)}\cdot 2R_{is}\cdot\cos\theta, \\
F'_{i\text{-els}}(t) &= \frac{4}{3}E_{\text{eq}}R_{\text{eq}}^{1/2}\left(\delta'_{2is}+\delta'_{3ib}\right)^{3/2}, \\
&\qquad \left(\delta'_{2is}+\delta'_{3ib} < \delta_y,\ \dot{\delta}'_{2is}+\dot{\delta}'_{3ib} > 0\right), \\
F'_{i\text{-pla}}(t) &= F_y + \pi A_y R_{\text{eq}}\sigma_y\left(\delta'_{2is}+\delta'_{3ib}-\delta_y\right), \\
&\qquad \left(\delta_y < \delta'_{2is}+\delta'_{3ib},\ \dot{\delta}'_{2is}+\dot{\delta}'_{3ib} > 0\right), \\
p'_{ci}(t) &= \frac{4F'_{i\text{-els}}(t)}{\pi a'^2_{2is}(t)}, \quad \left(\delta'_{2is}+\delta'_{3ib} < \delta_y\right), \\
p'_{ci}(t) &= \frac{4F'_{i\text{-pla}}(t)}{\pi a'^2_{2is}(t)}, \quad \left(\delta_y < \delta'_{2is}+\delta'_{3ib}\right), \\
a'_{2is}(t) &= \sqrt{\left(\delta'_{2is}+\delta'_{3ib}\right)\left(2R_{is}-\delta'_{2is}+\delta'_{3ib}\right)},
\end{aligned} \tag{15}$$

where $\cos\theta = \sqrt{(1-2\mu_f^2)/2(1-\mu_f'^2)}$, μ_f is the frictional coefficient between particle and the drop weight, and μ'_f is the frictional coefficient between particles.

$$\overline{v}'_i = \frac{3\beta}{2\pi}\left[a'_{2is}(t)\,\dot{\vartheta} + \vartheta\dot{a}'_{2is}(t)\right], \tag{16}$$

where $\beta = 8(1-\upsilon)/[3G(2-\upsilon)]$, $\vartheta = |\tau_{\max} - \tau_0| - \mu'^2_f p'^2_{ci}$, $\tau_{\max} = (1/2)p'_{ci}\sqrt{1+4\mu'^2_f}$, τ_0 is the critical shear stress, and for a free surface $\tau_0 = 0$.

The kinetic energy of drop weight is converted into the plastic work and friction heat of the particles:

$$\begin{aligned}
\dot{W}_{\text{sample}} &= \sum_{i=1}^{i=4}\frac{N}{2}\frac{C^1_{N_{1i}}C^1_{N_{2i}}}{C^2_N} \\
&\quad\cdot\int_0^{t_{\text{load}}}\left(p_{ci}\pi a^2_{1is}\dot{\delta}_{1is} + \mu_f p_{ci}\pi a^2_{1is}\overline{v}\right)dt \\
&\quad+\sum_{i=1}^{i=4}\frac{N}{2}\frac{C^1_{N_{1i}}C^1_{N_{2i}}}{C^2_N} \\
&\quad\cdot\int_0^{t_{\text{load}}}\left(p'_{ci}\pi a'^2_{2is}\left(\dot{\delta}'_{2is}+\dot{\delta}'_{3ib}\right) + \mu'_f p'_{ci}\pi a'^2_{2is}\overline{v}'_i\right)dt \\
&\quad= f_{\text{eff}}\int_0^{t_{\text{load}}} M_W\dot{x}_u\ddot{x}_u dt,
\end{aligned} \tag{17}$$

where f_{eff} is energy conversion coefficient.

The drop weight begins to rebound when the velocity decreases to zero. In this model, we do not pay attention to rebound stage. During the loading process, the velocity and displacement of drop weight should satisfy the following equation:

$$\dot{x}_u\big|_{t=t_{\text{load}}} = V_0 + gt_{\text{load}} - \frac{1}{M_W}\cdot\int_0^{t_{\text{load}}} F_c(t)\,dt, \tag{18}$$

$$\begin{aligned}
x_u\big|_{t=t_{\text{load}}} &= x_u\big|_{t=0} \\
&\quad+\int_0^{t_{\text{load}}}\left(V_0 + gt - \frac{1}{M_W}\cdot\int_0^{t_{\text{load}}} F_c(t)\,dt\right)dt.
\end{aligned} \tag{19}$$

During the process of impact, there are 21 unknowns, namely, h, x, F_c, F_i, d_s, v_p, p_{ci}, δ_{1i}, δ_{2i}, δ_{3i}, δ_{4i}, a_{1i}, a_{2i}, a_{3i}, a_{4i}, t_{load}, p'_{ci}, δ'_{2is}, δ'_{3ib}, a'_{2is}, and v'_i, and it is very difficult to get their values. Firstly, supposing that the samples are composed of the mean size particles, we use (1)–(3), (7)–(10), (14), and (18) to get h, x, d_s, F_c, v_p, and t_{load}. We assume that the force exerted on the each particles is equal; then we use (2)–(6) and (9)–(17) to get p_{ci}, δ_{1i}, δ_{2i}, δ_{3i}, δ_{4i}, a_{1i}, a_{2i}, a_{3i}, a_{4i}, p'_{ci}, δ'_{2is}, δ'_{3ib}, a'_{2is}, and v'_i.

2.3. Heat Equations of Hot Spot Sources

2.3.1. Hot Spots Source between Particle and Hammer Surface. During the impact process, the contact areas between particles and between the particles and the surface will form

potential "hot spots" due to plastic work and frictional heat. We suppose that potential hot spots are independent and small compared with the impacting drop weight surface. All the hot spots temperature calculations are only valid during the loading period t_{load}.The first kind of potential hot spot sources is from the contact points between the particles and the surface of drop weight. At time t, the rate of heat production per unit area is given by

$$\dot{q}_{1i}(t) = p_{ci}(t)\,\dot{\delta}_{1is}(t) + \mu_f p_{ci}(t)\,\overline{v}_p. \tag{20}$$

The energy density rate $\dot{q}_{1i}(t)$ actually results from the plastic work and the frictional heat. Given that the impression depth $\delta_{1is}(t)$ has been decomposed into elastic and plastic parts, the plastic part dominantly contributes to the temperature of contact points. We assume that $p_{ci}(t)$ is uniformly distributed along the frictional interface, and thus the mean radial velocity $\overline{v}_p$ is used instead of the radial velocity distribution. Herein, we assume that the total plastic work and frictional energy are dissipated into heat. By integrating the solutions for point sources with respect to appropriate space variables, we obtain solutions for temperature increasing at the center of the contact interface because of the amount of heat $q_{1i}\pi a_{1is}^2$ liberated during time from 0 to t_{load} over a disk of radius $a_{1is}(t)$. The temperature ΔT_{1i} at the interface after a time interval of t_{load} can be obtained by Carslaw and Jaeger [25]:

$$\begin{aligned}\Delta T_{1i}(t) = {} & \frac{1}{2\rho_s C\sqrt{\pi\kappa}} \times \int_0^{t_{\text{load}}} \frac{\dot{q}_{1i}(t)}{\left(t_{\text{load}} - t\right)^{1/2}} \left[1 \right. \\ & \left. - \exp\left\{-\frac{a_{1is}^2(t)}{4\kappa\left(t_{\text{load}} - t\right)}\right\}\right] dt \\ & + \int_0^{t_{\text{load}}} \frac{\mu_f p_{ci}(t)\,\overline{v}_r}{2\sqrt{\pi\kappa t}} dt.\end{aligned} \tag{21}$$

2.3.2. Hot Spot Sources between Particles. The hot spot sources between particles are a result of the plastic work and the frictional heat among particles surfaces with a relative sliding. These hot spot sources may devote more to ignition than that between particles and hammer surface, because they are in the interior of the sample. At time t, the rate of heat production per unit area $\dot{q}_{2i}(t)$ and temperature ΔT_{2i} of the hot spot sources between particles are given by [26]

$$\dot{q}_{2i}(t) = p'_{ci}(t)\left(\dot{\delta}'_{2is}(t) + \dot{\delta}'_{3ib}(t)\right) + \mu'_f p'_{ci}(t)\,\overline{v}'_i, \tag{22}$$

$$\begin{aligned}\Delta T_{2i}(t) = {} & \frac{1}{2\rho_s C\sqrt{\pi\kappa}} \times \int_0^{t_{\text{load}}} \frac{\dot{q}_{2i}(t)}{\left(t_{\text{load}} - t\right)^{1/2}} \left[1 \right. \\ & \left. - \exp\left\{-\frac{a'^2_{2is}(t)}{4\kappa\left(t_{\text{load}} - t\right)}\right\}\right] dt \\ & + \int_0^{t_{\text{load}}} \frac{\mu'_f p'_{ci}(t)\,\overline{v}'_i}{2\sqrt{\pi\kappa t}} dt.\end{aligned} \tag{23}$$

For energetic materials, the temperature raise should include chemical heat. A single step zero order Arrhenius reaction is applied:

$$\dot{Q} = q_r Z_r \exp\left(\frac{-E_A}{R_g T}\right). \tag{24}$$

Therefore, the temperature increase terms contributed by the heat of the chemical reaction should be added to (21) and (23), which is

$$\Delta T_{\text{chem}} = \int_0^{t_{\text{load}}} \frac{1}{c} q_r Z_r \exp\left(\frac{-E_A}{R_g T}\right) dt, \tag{25}$$

where Z_r is the preexponential factor, E_A is the activation energy, q_r is the heat of reaction per unit mass for a single step chemical decomposition, and R_g is the universal gas constant. When $\Delta T \le T_{\text{melt}}$, the contact zones are solid. However, a liquid-solid phase transition is initiated when the temperature at the contact zone reaches the melting point. The temperature remains at the melting point $\Delta T_i = T_{\text{melt}}$ and part of the heat is consumed in the phase transition during the melting process. The endothermic heat rate from solid to liquid per unit volume is taken into account:

$$\dot{Q}_{S\to L} = \rho_s q_\lambda \dot{\varphi}_L, \tag{26}$$

where $\dot{\varphi}_L$ is the volume fraction of liquid and q_λ is the latent heat per unit mass, which can be calculated from the rate of heat generation per mass by

$$\dot{\varphi}_L = \frac{\dot{q}}{\delta\rho_s q_\lambda}. \tag{27}$$

The potential hot spots either fail to react due to thermal diffusion or react exothermically, allowing potential hot spots to increase in temperature and size after drop weight impact.

2.4. Ignition Probability. If the potential hot spots satisfy critical conditions of hot spots, the potential hot spot became a real hot spot. The critical temperature of hot spots is 700 K [27]. The real hot spot will grow and coalesce with other hot spots which results in particles combustion, even explosion. The formation of a real hot spot means ignition. Because of the different sizes of particles, the temperature of potential hot spots is different too. In the experiment, the total number of potential hot spots is much less than that in the theoretical model, so we provide a coefficient η to revise the total number of potential hot spots. The hot spots will be formed among some potential hot spots and will not be formed among others. Since the probability of potential hot spots is based on the particle size and distribution, the ignition probability is the function of particle size and distribution. Ignition probability is defined as follows:

$$\begin{aligned}P_{\text{ignition}} & \\ & = \eta \\ & \cdot \left(N \cdot \chi_i \cdot \frac{\sum_{i=1}^{8} C_{N_i}^1}{C_N^1} + \frac{N}{2} \cdot \chi_j \cdot \frac{\sum_{j=1}^{8} C_{N_j}^1 C_{N_j}^1}{C_N^2}\right),\end{aligned} \tag{28}$$

Table 2: Material parameters of HMX particle.

Parameters for the calculations of HMX	HMX
Density (kg·m^{-3})	1910.0
Young modulus (GPa)	24.0
Shear modulus (GPa)	12.0
Poisson's ratio	0.322
Yield strength (MPa)	125.0
Friction coefficient between particles μ_f	0.251
Friction coefficient between particles and anvil μ_f'	0.196
Average particle radius (μm)	160.0
Range size α (μm)	20
Surface energies (mJ/m^2)	15.5
Specific heat (J·kg^{-1}·K^{-1})	1250.0
Thermal conductivity (J·m^{-1}·s^{-1}·K^{-1})	0.525
Reaction heat release per mass q_r (J·kg^{-1})	5.96e6
Prefrequency factor Z_r (s^{-1})	2.04e18
Activation energy E_A (J·mol^{-1})	2.055e5
Latent heat of fusion q_λ (J·kg^{-1})	2.2e5
Melting point T_m (K)	552.0

where $N \cdot \chi_i \cdot \sum_{i=1}^{8} C_{N_i}^1 / C_N^1$ is the probability of the formation of a real hot spot between particles and drop weight surface, N is the total number of potential hot spots between particles and drop weight surface, and χ_i is the coefficient for ignition probability. If the potential hot spot has not become a real hot spot, then $\chi_i = 0$; otherwise $\chi_i = 1$. In (28), $(N/2) \cdot \chi_j \cdot \sum_{j=1}^{8} C_{N_j}^1 C_{N_j}^1 / C_N^2$ is the probability of the formation of a real hot spot between particles, where $N/2$ is the total number of potential hot spots between particles, and χ_j is the coefficient for ignition probability. If the potential hot spot has not become a real hot spot, then $\chi_j = 0$; otherwise $\chi_j = 1$. The value of the coefficient is 0.10.

3. Calculated Results

To obtain the temperature between particles and between the particles and drop weight surface during impact, a series of calculations were performed. Parameters for the calculation in the impact process are listed in Table 2. Most material parameters reflect their physical properties, including density, specific heat, and Young and shear modulus. And we got the average particle radius from the experiments. Range size α is a parameter that we gave artificially.

3.1. Temperature of Contact Points. The study of the temperature history for the hot spot sources reveals their respective sensitivity to drop weight impact. Given that the mechanism of impact initiation possibly involves the formation of small regions of high temperature, the hot spots may serve as the nuclei from which the deflagration and detonation grow. The present model implies that the impact explosion can be treated as a two-step process. The hot spot is formed in the explosive during the first step, which is modeled in the present study. The second step, wherein the exothermic reaction within the hot spot leads to sustained deflagration and/or detonation, is not included in the present model.

In the process of drop weight impact, the contact areas between the particles and the drop weight surface and between particles become potential "hot spots" due to plastic work and frictional heat. After calculation, the temperature-time curves of different contact areas between the particles and the drop weight surface and between particles were obtained. The calculated results showed that the temperature of the contact zones was strongly dependent on the particles size and contact position. The temperature of contact position between particles and the drop weight surface increases faster and higher than that of the contact position between two neighboring particles. Figures 4(a)~4(d) represent the temperature-time curves between particles and drop weight surface under the weight of 5.0 kg and the heights are 0.1 m, 0.2 m, 0.3 m, and 0.4 m, respectively. The number in the picture represents the mean radius of the particles in each range. The smaller the size of particles is, the higher the temperature of the contact zones will be. We found that the contact zone between particles and drop weight surface is easy to ignite, so these contact positions have a great influence on the probability of the formation of a real hot spot. In this paper, ignition probability is the probability of the formation of a real hot spot, so the ignition probability strongly related to these contact positions.

Figures 5(a)~5(d) represent the temperature-time curves between particles under the weight of 5.0 kg and the heights are 0.1 m, 0.2 m, 0.3 m, and 0.4 m, respectively. The greater the size of two contacted particles is, the lower the temperature of the contact zones will be. We found that the contact zone between particles is not easy ignition, but this hot spot source may devote more to combustion in the powder explosive with stronger confinement or bulk explosive material.

3.2. Ignition Probability. Figure 6 shows the ignition probability of the experimental results and the calculation results in different drop height. In Figure 6 drop weights are all 5.0 kg and drop heights are 0.1 m, 0.2 m, 0.3 m, and 0.4 m, respectively. Figure 6 shows that there is a significant increase of ignition probability with the increase of drop height. If the height of the drop weight is less than 0.1 m, the temperature of all contact zones is lower than critical temperature of the hot spots and no hot spots have been formed; then ignition probability will be close to 0. With the increase of the drop height, the temperature of contact zone is also increased, and then some potential hot spot may become a real hot spot which means ignition. Therefore, we reasonably defined ignition probability as the probability of the formation of a real hot spot. The probability of forming a real hot spot is 0.104 under the drop height of 0.2 m. When the drop heights are 0.3 m and 0.4 m, the probability of forming a real hot spot is 0.657 and 0.989, respectively, which is slightly lower than the experimental data. The experimental results exhibit a similar trend with the calculation results, indicating that our model is reasonable.

4. Conclusion

In this paper, based on the distribution of micron scale explosive particles, a microscopic model is established to

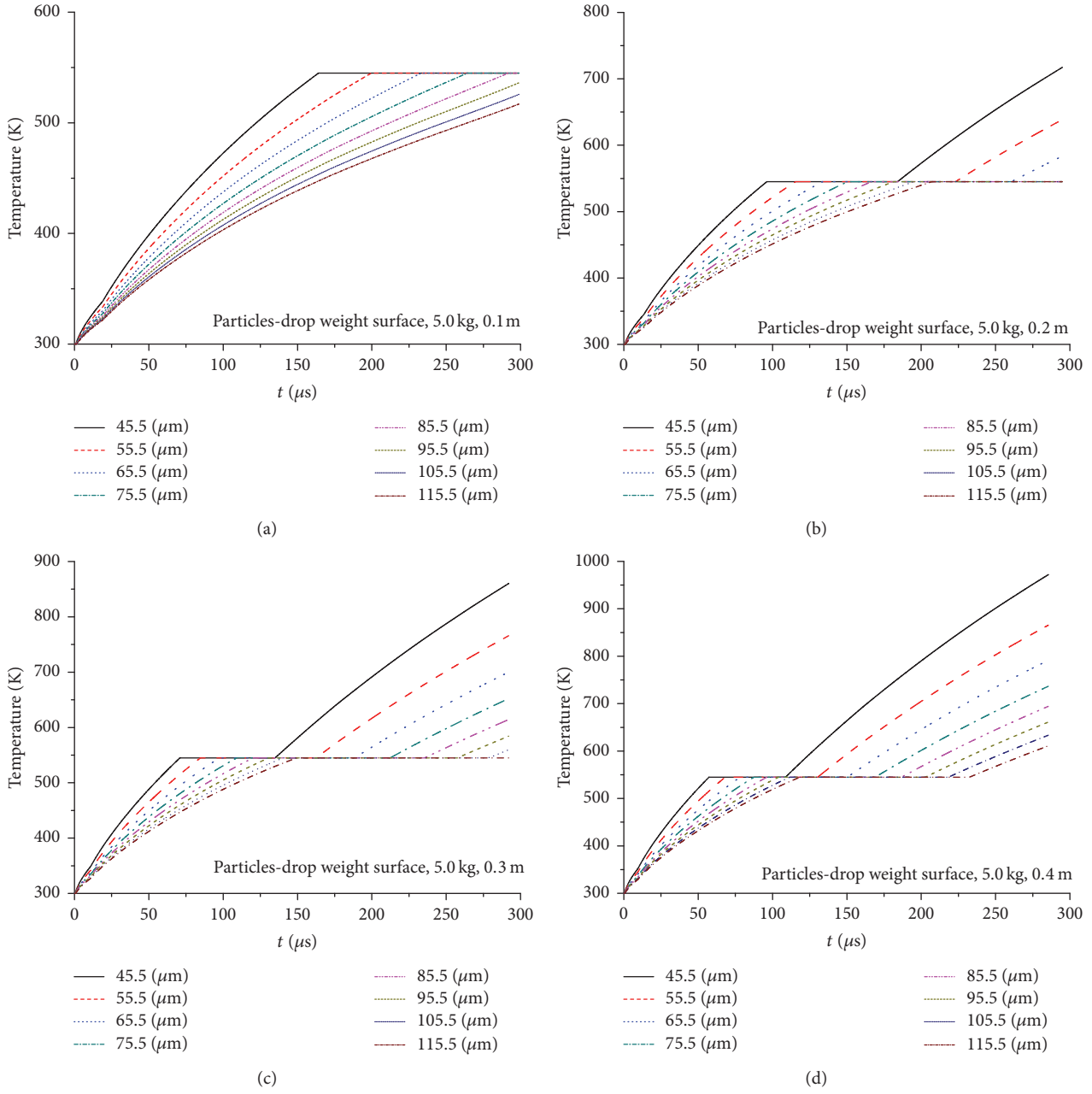

Figure 4: (a)~(d) represent the temperature-time curves between different-sized particles and hammer under the weight of 5.0 kg and the heights are 0.1 m, 0.2 m, 0.3 m, and 0.4 m, respectively.

describe the process of ignition of HMX particles. The key feature of our model is the microparticle contact deformation between two unequal-sized particles. The present model has been used to evaluate the ignition probability of explosive particles under drop height. The size and distribution of the particles are investigated by Laser Particle Size Analyzer Malvern MS2000 before experiment and calculation. The mean size of particles is 161 μm. Minimum and maximum sizes are 80 μm and 263 μm, respectively. The distribution function is like a quadratic function. We theoretically calculated the plastic work and friction heat of the contact points (in the impact process) of different particle size and obtained the temperature-time curve of the contact points. The results show that the temperature of the contact point between particles and drop weight surface is higher and increases faster than that between two neighboring particles. By analyzing the probability distribution of particle size, we get the ignition probability. For HMX particles, with all other conditions being kept constant, if the drop height is less than 0.1 m, ignition probability will be close to 0. When the drop heights are 0.2 m and 0.3 m, the ignition probability is 0.27 and 0.64, respectively. When the drop height is more than 0.4 cm, ignition probability will be close to 0.82. In comparison with experimental results, the two curves are

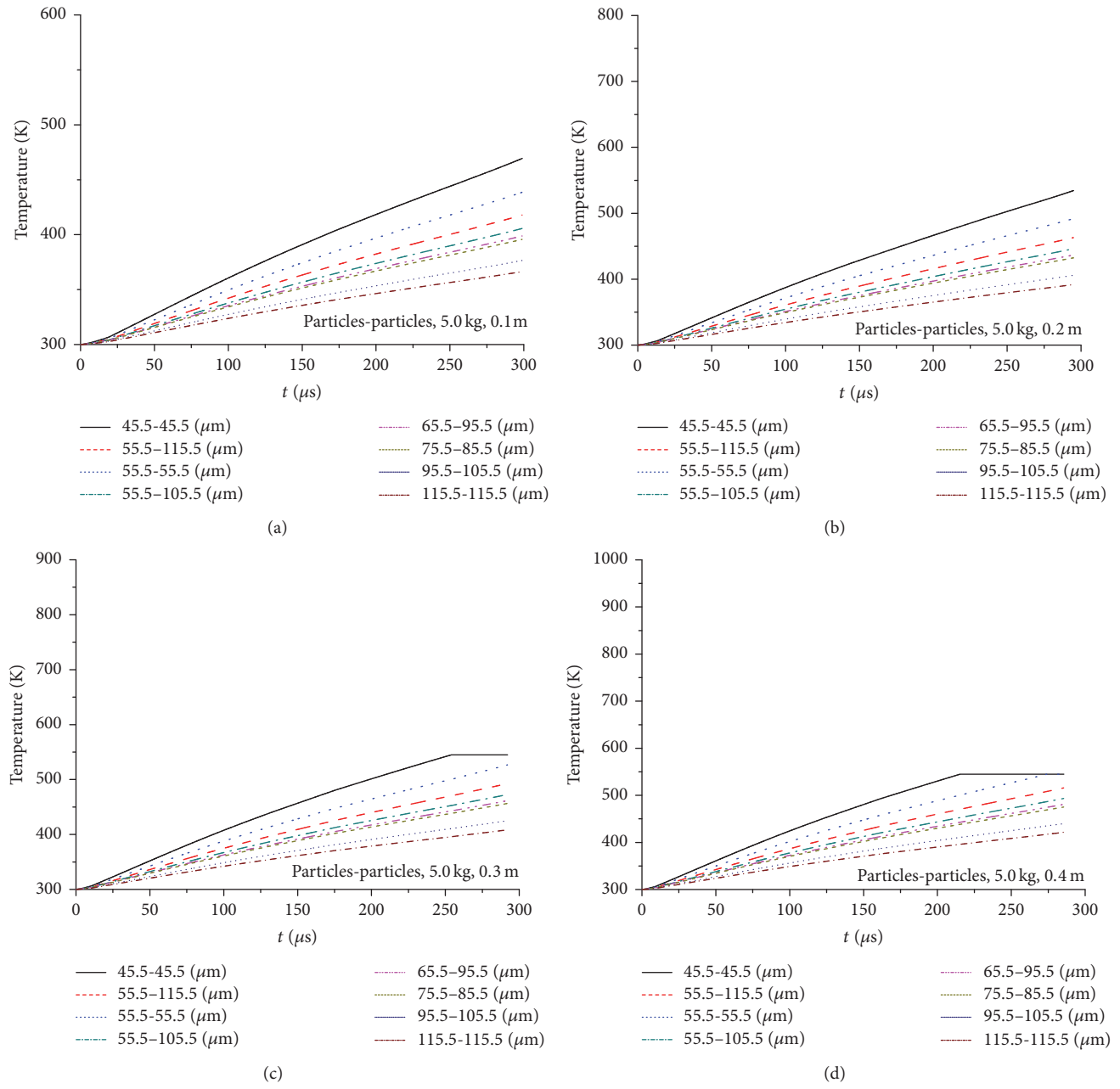

FIGURE 5: (a)~(d) represent the temperature-time curves between different-sized particles under the weight of 5.0 kg and the heights are 0.1 m, 0.2 m, 0.3 m, and 0.4 m, respectively.

reasonably close to each other, indicating that our model has a certain degree of rationality.

The simulation errors mainly come from the uncertainty of the number of potential hot spots. The number of theoretically potential hot spots is larger than that of potential hot spots in the experiment. In this paper, we use the revised number of theoretically potential hot spots to calculate the ignition probability. If the particle is smaller, it easily falls into the space among the larger particles, which reduces the number of potential hot spots and the corresponding ignition probability. And if the particle size is bigger, the particle is not easy to fall into the space among smaller particles, and the number of potential hot spots may have a certain increase, which also improves the ignition probability. Of course, the model of this paper is a simplified one in which many issues are ignored. Firstly, HMX has several phases: α, β, δ, ε, and ϕ. When the temperature is increased above 175°C, the phase transfers from α to β. When HMX is heated above 435 K, a phase transition of β to δ is happened. Energy conversion of the phase change process is not included in the model. Secondly, in the process of drop weight impact, wave propagation, and reflection, refraction is a very complicated process, which has not been considered in detail. Thirdly, phase conversion of material from solid to liquid and liquid

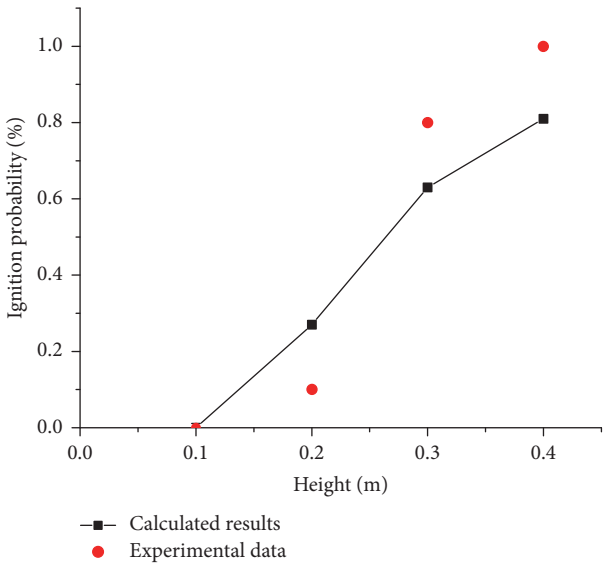

FIGURE 6: The figure shows the ignition probability of the experimental results and the calculation results in different drop height.

combustion have not been given a complete description. Fourthly, we consider the size of particle in the model, but the shape of particle will also affect the formation of hot spots. Finally, the growth and coalescence of hot spots and particle combustion are not included in the model.

The primary objective of the present study is to establish a full theoretical framework for predicting mechanical and thermal responses at the particle level in a drop weight impact event. In the future research, the phase transfers of explosive under drop weight, the wave propagation, the growth and coalescence of hot spot, and granular combustion will be studied.

Competing Interests

The authors declare that there is no conflict of interests regarding the publication of this paper.

Acknowledgments

The authors would like to thank the Chinese National Nature Science Foundation (Grant nos. 11572045 and 11472051) and Science Challenge Project (JCKY2016212A501) and Open Funding from Center for Research and Development of Safety Ammunition (RMC2015B03) for supporting this project.

References

[1] P. J. Baker and A. M. Mellor, "Energetic materials impact initiation mechanisms," *Combustion Science and Technology. Book Series*, vol. 4, pp. 289–316, 1997.

[2] K. L. McNesby and C. S. Coffey, "Spectroscopic determination of impact sensitivities of explosives," *Journal of Physical Chemistry B*, vol. 101, no. 16, pp. 3097–3104, 1997.

[3] S. N. Heavens and J. E. Field, "The ignition of a thin layer of explosive by impact," *Proceedings of the Royal Society A: Mathematical, Physical & Engineering Sciences*, vol. 338, no. 1612, pp. 77–93, 1974.

[4] H. Czerski, M. W. Greenaway, W. G. Proud, and J. E. Field, "β-δ phase transition during dropweight impact on cyclotetramethylene-tetranitroamine," *Journal of Applied Physics*, vol. 96, no. 8, pp. 4131–4134, 2004.

[5] Y. Zhang, C. Lv, D. Liu, L. Guo, and T. Fu, "Preparation of microcrystals of organic compounds with polar groups and inorganic salts by reprecipitation," *Japanese Journal of Applied Physics, Part 1: Regular Papers & Short Notes and Review Papers*, vol. 44, no. 7, pp. 5319–5321, 2005.

[6] Y.-Q. Wu and F.-L. Huang, "Experimental investigations on a layer of HMX explosive crystals in response to drop-weight impact," *Combustion Science and Technology*, vol. 185, no. 2, pp. 269–292, 2013.

[7] C.-W. An, X.-D. Guo, W.-X. Xie, X.-L. Song, Y. Wang, and F.-S. Li, "Preparation and mechanical sensitivity of HMX/HTPB composite particles," *Journal of Nanjing University of Science & Technology*, vol. 33, no. 2, pp. 267–271, 2009.

[8] G. Zhang and B. L. Weeks, "A device for testing thermal impact sensitivity of high explosives," *Propellants, Explosives, Pyrotechnics*, vol. 35, no. 5, pp. 440–445, 2010.

[9] J. Namkung and C. S. Coffey, "Plastic deformation rate and initiation of crystalline explosives," *Shock Compression of Condensed Matter*, vol. 1003, pp. 1003–1006, 2001.

[10] M. H. Keshavarz and M. Jaafari, "Investigation of the various structure parameters for predicting impact sensitivity of energetic molecules via artificial neural network," *Propellants, Explosives, Pyrotechnics*, vol. 31, no. 3, pp. 216–225, 2006.

[11] F. Huang and Y. Wu, "Hot-spot ignition in a layer of widely-spaced HMX powders subjected to a falling weight impact," in *Proceedings of the Biennial International Conference of the Aps Topical Group on Shock Compression of Condensed Matter*, 2011.

[12] Y. Q. Wu, F. L. Huang, and M. Huang, "Modeling of ignition in a single layer of impacted energetic crystals," *Propellants Explosives Pyrotechnics*, vol. 35, pp. 1–10, 2010.

[13] Y.-Q. Wu and F.-L. Huang, "A microscopic model for predicting hot-spot ignition of granular energetic crystals in response to drop-weight impacts," *Mechanics of Materials*, vol. 43, no. 12, pp. 835–852, 2011.

[14] Y. Q. Wu, F. L. Huang, and M. Zhou, "Microscopic modeling of ignition and burning for well-arranged energetic crystals in response to drop-weight impact," *Journal of Physics: Conference Series*, vol. 58, no. 7, 2014.

[15] K. S. Adegbie and F. I. Alao, "Studies on the effects of interphase heat exchange during thermal explosion in a combustible dusty gas with general Arrhenius reaction-rate laws," *Journal of Applied Mathematics*, vol. 2012, Article ID 541348, 15 pages, 2012.

[16] A. Jankowski, "Modelling of combustion processes of liquid fuels," *Journal of KONES. Powertrain and Transport*, vol. 19, no. 4, pp. 239–244, 2012.

[17] D. O. Glushkov, G. V. Kuznetsov, and P. A. Strizhak, "Numerical and experimental research of heat and mass transfer at the heterogeneous system ignition by local energy source with limited heat content," *Mathematical Problems in Engineering*, vol. 2014, Article ID 281527, 7 pages, 2014.

[18] O. V. Vysokomornaya, G. V. Kuznetsov, and P. A. Strizhak, "Mathematical simulation of heat and mass transfer processes

at the ignition of liquid fuel by concentrated flux of radiation," *Mathematical Problems in Engineering*, vol. 2014, Article ID 156150, 7 pages, 2014.

[19] S. D. Nemoda, M. R. Mladenović, M. J. Paprika, A. M. Erić, and B. D. Grubor, "Three phase eulerian-granular model applied on numerical simulation of non-conventional liquid fuels combustion in a bubbling fluidized bed," *Thermal Science*, vol. 20, pp. s133–s149, 2016.

[20] K. L. Johnson, *Contact Mechanics: Normal Contact of Elastic Solids-Hertz Theory*, vol. 89, Cambridge University Press, New York, NY, USA, 1985.

[21] C. Thornton and Z. Ning, "A theoretical model for the stick/bounce behaviour of adhesive, elastic- plastic spheres," *Powder Technology*, vol. 99, no. 2, pp. 154–162, 1998.

[22] L. M. Tavares and R. P. King, "Single-particle fracture under impact loading," *International Journal of Mineral Processing*, vol. 54, no. 1, pp. 1–28, 1998.

[23] C. M. Segedin, "Note on a penny-shaped crack under shear," *Mathematical Proceedings of the Cambridge Philosophical Society*, vol. 47, pp. 396–400, 1951.

[24] J. K. Dienes, Q. H. Zuo, and J. D. Kershner, "Impact initiation of explosives and propellants via statistical crack mechanics," *Journal of the Mechanics & Physics of Solids*, vol. 54, no. 6, pp. 1237–1275, 2006.

[25] H. S. Carslaw and J. C. Jaeger, *Conduction of Heat in Solids*, Clarendon Press, Oxford, UK, 1959.

[26] H. Czerski, *Ignition of HMX and RDX*, University of Cambridge, 2006.

[27] F. P. Bowden, A. D. Yoffe, and G. E. Hudson, "Initiation and growth of explosion in liquids and solids," *American Journal of Physics*, vol. 20, no. 4, pp. 250–251, 1952.